

See discussions, stats, and author profiles for this publication at: <https://www.researchgate.net/publication/231679490>

Measurements of Interfacial Curvatures of Bicontinuous Structure from Three-Dimensional Digital Images. 1. A Parallel Surface Method

ARTICLE *in* LANGMUIR · JANUARY 1998

Impact Factor: 4.46 · DOI: 10.1021/la970868b

CITATIONS

64

READS

7

5 AUTHORS, INCLUDING:



Hiroshi Jinnai

Tohoku University

234 PUBLICATIONS 4,238 CITATIONS

[SEE PROFILE](#)



Takeji Hashimoto

Kyoto University

517 PUBLICATIONS 17,172 CITATIONS

[SEE PROFILE](#)



S. T. Hyde

Australian National University

158 PUBLICATIONS 5,369 CITATIONS

[SEE PROFILE](#)

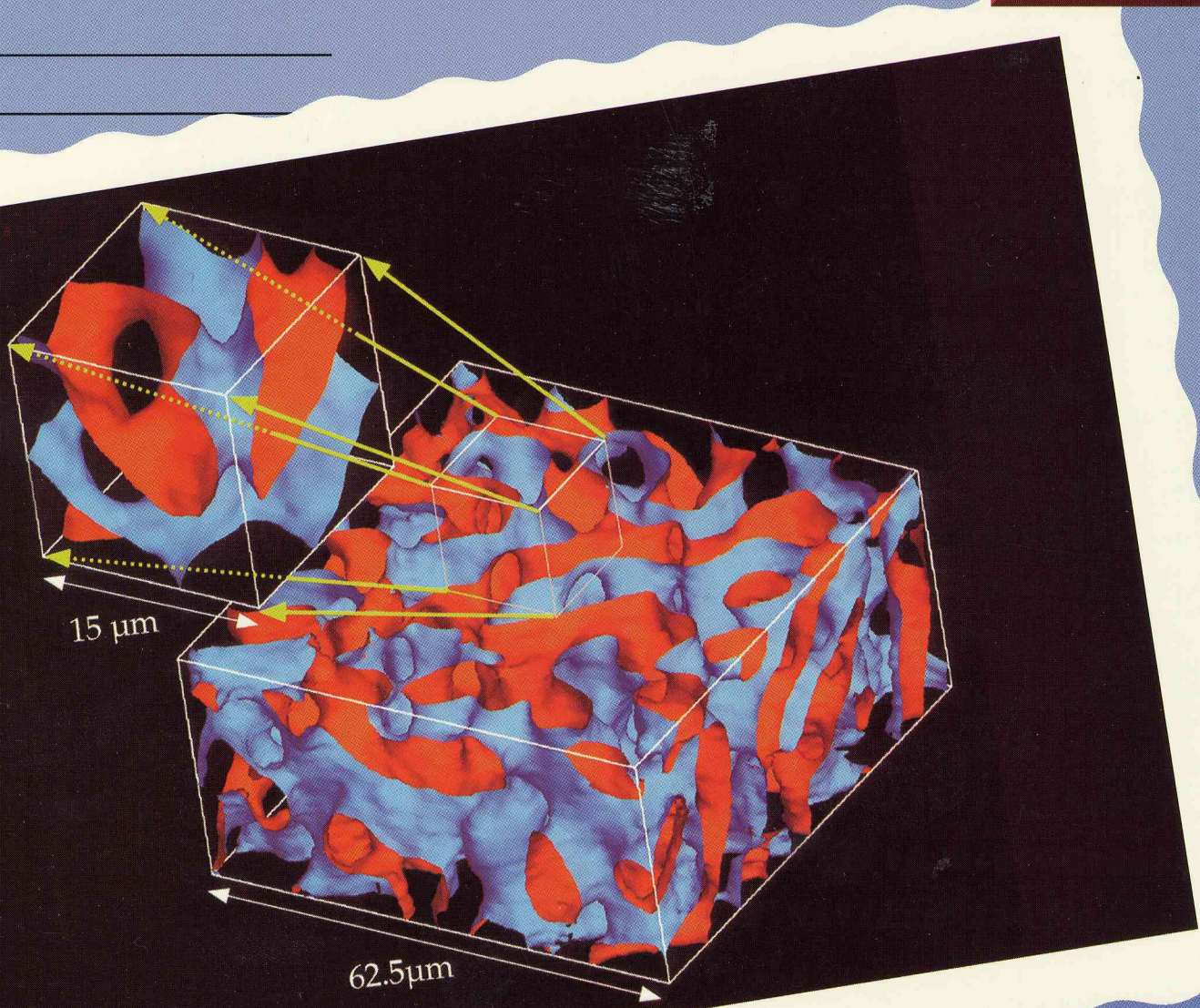
Langmuir

The ACS Journal of Surfaces and Colloids

MARCH 3, 1998

VOLUME 14, NUMBER 5

AVAILABLE
ON THE WEB
<http://pubs.acs.org>



Interface of a Phase Separated
Mixture in Three Dimensions.
(see p. 1242)

Measurements of Interfacial Curvatures of Bicontinuous Structure from Three-Dimensional Digital Images. 1. A Parallel Surface Method

Yukihiro Nishikawa,[†] Hiroshi Jinnai,^{*,†} Tsuyoshi Koga,[†]
Takeji Hashimoto,^{*,†,‡} and Stephen T. Hyde[§]

Hashimoto Polymer Phasing Project, ERATO, JST, Keihan-na Plaza, 1-7 Hikari-dai, Seika, Kyoto 619-02, Japan, and Department of Polymer Chemistry, Graduate School of Engineering, Kyoto University, Kyoto 606-01, Japan, and Applied Mathematics Department, Research School of Physical Sciences, Australian National University, Canberra 0200, Australia

Received August 4, 1997. In Final Form: October 15, 1997

A method was developed to measure the area-averaged mean and the Gaussian curvatures from three-dimensional (3D) digital images of the interface of complicated bicontinuous structures. This method involves measurement of areas of surfaces that are parallel to the interface as a function of displacement from it. The applicability and precision of the scheme were critically examined by using a known minimal surface, i.e., the gyroid, as a model of bicontinuous structures. The method was then applied to 3D images of the interface of the phase-separated bicontinuous structure of a *real* polymer blend in order to evaluate the characteristic of curvatures of the interface.

1. Introduction

Bicontinuous structures are commonly formed in a variety of condensed materials. As equilibrium structures, they are formed in microphase-separated block copolymers¹ and in microemulsions.^{2,3} Block copolymers, abbreviated A-*b*-B, consist of two different types of polymers, A and B, connected by a covalent bond. Bicontinuous structures are also formed, as nonequilibrium structures, in the course of a phase separation process called spinodal decomposition (SD), in binary mixtures of polymers (polymer blends), simple fluid mixtures, metallic alloys, and inorganic glasses.^{4,5} A considerable number of studies of SD have been done, because the process is a typical example of nonlinear and nonequilibrium phenomena. We call the interface of such bicontinuous structures *a bicontinuous interface*.

In the case of A-*b*-B block copolymers, it is reported that the bicontinuous microphase-separated structures, are formed over a narrow range of volume fraction of one of the constituents.^{1,6–8} The bicontinuous interface between the two microdomains, i.e., domains consisting of A and B polymers, appears because of the preferred spontaneous curvature which is realized due to the requirement of the uniform density distribution of the block copolymers in space (incompressibility). The bicontinuous interfaces in block copolymers are often conveniently modeled by a gyroid, one of the minimal surfaces of the differential geometry.^{7,8} However, almost no data are available to support the model of the interface

as a true minimal surface, although the microdomain topology does appear to follow that of a gyroid.⁸ Measurement of interfacial curvatures, i.e., the mean, H , and the Gaussian, K , curvatures (defined later in eq 1), and their distributions offers insight into the exact geometry of the interface, in particular, whether it is truly minimal (of zero mean curvature) or not. We note, quite recently, three-dimensional (3D) imaging of a linear triblock of polystyrene-block-polyisoprene-block-polystyrene (SIS) using transmission electron microtomography⁹ has been reported, in which the cubic bicontinuous morphology with $Ia\bar{3}d$ symmetry of the SIS triblock copolymer was demonstrated.⁹ Curvature (distribution) measurements of such 3D images should offer a direct way to examine the validity of the assumption of using the minimal surface as the model to describe the bicontinuous structures in block copolymer systems.

In microemulsions, the surfactants in ternary mixtures of oil/water/surfactant form monolayers at the interfaces between oil and water.² Under certain conditions, the surfactants are self-assembled into the bicontinuous interface. Moreover, polymeric bicontinuous microemulsions which consist of binary or ternary block copolymer/homopolymer(s) have also been reported.^{10,11} The system is often considered as an idealized surface with negligible interfacial tension, so that its free energy is dominated by curvature energies, which can be estimated from interfacial curvatures.¹² In such a theory, the interplay between the bending rigidities of the surfactant monolayers and the statistical fluctuations of the interface determines the topology of the system. On the other hand,

* To whom correspondence should be addressed.

[†] Hashimoto Polymer Phasing Project, ERATO, JST.

[‡] Kyoto University.

[§] Australian National University.

(1) Thomas, E. L.; Anderson, D. B.; Henkee, C. S.; Hoffman, D. *Nature* **1988**, *334*, 598.

(2) Jahn, W.; Strey, R. *J. Phys. Chem.* **1988**, *92*, 2294.

(3) Chen, S. H.; Chang, S. L.; Strey, R., *J. Chem. Phys.* **1990**, *93*, 1907.

(4) Gunton, J. D.; San Miguel, M.; Sahni, P. S. *Phase Transitions and Critical Phenomena*; Domb, C., Lebowitz J. L., Eds.; Academic Press: New York, 1983; Vol. 8.

(5) Hashimoto, T. In *Structure and Properties, Materials Science and Technology*; Thomas, E. L., Ed.; VCH: Weinheim, 1993; Vol. 12.

(6) Hasegawa, H.; Tanaka, H.; Yamasaki, K.; Hashimoto, T. *Macromolecules* **1987**, *20*, 1651.

(7) Hasegawa, H.; Nishikawa, Y.; Koizumi, S.; Hashimoto, T.; Hyde, S. T. In *Advanced Materials '93, II/A: Biomaterials, Organic and Intelligent Materials*; Aoki, H., et al. Eds.; Elsevier Science B.V.: Amsterdam, 1993.

(8) Hajduk, D. A.; Harper, P. E.; Gruner, S. M.; Honeker, C. C.; Kim, G.; Thomas, E. L.; Fetter, L. *J. Macromolecules* **1994**, *27*, 4063.

(9) Laurer, J. H.; Hajduk, D. A.; Fung, J. C.; Sedat, J. W.; Smith, S. D.; Gruner, S. M.; Agard, D. A.; Spontak, R. *J. Macromolecules* **1997**, *30*, 3938.

(10) Laurer, J. H.; Fung, J. C.; Sedat, J. W.; Smith, S. D.; Samseth, J.; Mortensen, K.; Agard, D. A.; Spontak, R. *J. Langmuir* **1997**, *13*, 2177.

(11) Bates, F. S.; Maurer, W. W.; Lipic, P. M.; Hillmyer, M. A.; Almdal, K.; Mortensen, K.; Fredrickson, G. H.; Lodge, T. P. *Phys. Rev. Lett.* **1997**, *79*, 849.

the interfacial curvatures are also significant parameters¹³ for the transient structures formed during SD. The rate of the domain growth in late stage SD is described by the interfacial curvatures. Thus, measurement of the curvatures is essential, in that they quantify the coarsening process. However, to our knowledge, few attempts to measure the curvatures of bicontinuous interfaces have been made with the exception of scattering experiments.^{14–16}

Lee et al.¹⁴ measured the area-averaged mean curvature of the surfactant monolayers in microemulsions by small-angle neutron scattering (SANS), using a contrast variation method. They varied the scattering length density of oil and water by deuterium labeling to estimate water–surfactant and oil–surfactant interfacial areas, whose difference can be used to calculate the curvatures. However, in practice, smearing effects due to the interpenetration of oil or water into the surfactant monolayer and experimental errors made the measurement of K of the system too difficult to implement. Chen et al.¹⁵ assumed the geometry of the surfactant monolayers was described by a random Gaussian wave (RGW) model,¹⁷ thereby estimating the interfacial curvatures of the surfactant monolayer. The RGW model was recently applied to a polymer blend to estimate the interfacial curvatures.¹⁶ To date then, attempts to measure interfacial curvatures using scattering are less than complete: they either lack sufficient accuracy in the data or rely on an assumed model geometry.

A direct method to determine the curvatures of these complex structures is to analyze two-dimensional (2D) or three-dimensional (digital) images, since this approach does not rely on any model of geometry. Some authors have tried to estimate curvatures from (digital) images such as those obtained by microscopy. Läuger et al. attempted to estimate the interfacial curvature of a phase-separated polymer mixture undergoing SD.¹⁸ They manually picked a representative curvature of the interface from their microscopic images of the phase-separated structures, which may be useful in some limited cases. The curvature thus obtained agreed with those estimated from scattering function on the basis of Tomita's theory.¹⁹ However, the microscope images were 2D slices of the 3D bicontinuous structure and, hence, the inferred curvature had 2D rather than 3D nature. Moreover, the curvature was not a statistically averaged value, i.e., area-averaged quantity, which should be the case in Tomita's theory. It is worth noting that the method to estimate the curvature from the scattering function which Läuger et al. relied on seems to be incorrect.²⁰ A similar but more quantitative discussion has been given by Kawakatsu et al. for their 2D computer-simulated images, in which they dealt with effects of additive surfactant on the interfacial curvature in the liquid/liquid phase separation.²¹

Determination of the interfacial curvatures from digital images can be a general topic of interest in image processing. Besl et al.²² proposed a method to obtain

- (12) Mutz, M.; Helfrich, W. *J. Phys. (Paris)* **1990**, *51*, 991.
- (13) Cahn, J. W. *Trans. Metall. Soc. AIME* **1967**, *239*, 610.
- (14) Lee, D. D.; Chem, S. H. *Phys. Rev. Lett.* **1994**, *73*, 106.
- (15) Chen, S. H.; Lee, D. D.; Chan, S. L. *J. Mol. Struct.* **1993**, *296*, 256.
- (16) Jinnai, H.; Hashimoto, T.; Lee, D. D.; Chen, S. H. *Macromolecules* **1997**, *30*, 130.
- (17) Berk, N. F. *Phys. Rev. A* **1991**, *44*, 5069.
- (18) Läuger, J.; Lay, R.; Maas, S.; Gronski, W. *Macromolecules* **1995**, *28*, 7010.
- (19) Tomita, H. *Prog. Theor. Phys.* **1984**, *72*, 656.
- (20) Jinnai, H.; Nishikawa, Y.; Koga, T.; Hashimoto, T. In *Interfacial Aspects of Multicomponent Polymer Materials*; Lohse, D. J., Russel, T. P., Sperling, L. H., Eds.; Plenum Press: New York, 1997; p 53.

curvature from 2D images whose intensity corresponds to the height of the pixels, such as a map. They estimated the interfacial curvatures by combining the first and second derivatives of the intensity between the neighboring pixels on the basis of *differential geometry*. Although this method may be useful to evaluate curvatures from the 2D images, these data are insufficient to probe the exact nature of the bicontinuous structures. Bullard et al.²³ analyzed local volume fractions of the inner and outer parts of the surface in the spherical “template” around a point of interest in order to obtain H . This technique, however, does not admit estimation of the complete structure; K cannot be obtained.

In the present paper, we describe a method to measure interfacial curvatures, i.e., both H and K from 3D digital images with the aid of equations from differential geometry. The method is applicable to any surface geometry, including bicontinuous morphologies. The method is applied to the 3D image of the bicontinuous interface of a *real* polymer blend developed in the course of an SD process^{24,25} obtained by laser scanning confocal microscopy (LSCM).²⁶ A quantitative discussion of the local structure of the interface, as well as its global topology, will be given later in the paper.

2. Principle and Method

Surface curvatures are fundamental parameters characterizing the shape of a surface. The curvatures at an arbitrary point on the surface can be expressed by two principal curvatures or the mean and Gaussian curvatures.²⁷ A two-dimensional curvature is defined for a planar curved path passing through a point of interest, \mathbf{p} , on the surface, whose plane contains the surface normal vector at the point (the bold italic letter designates a vector in 3D space). Paths with different tangential directions on the surface have, in general, different values for the curvatures. Maximum and minimum values among those curvatures at the point of interest are called the principal curvatures, i.e., κ_1 and κ_2 , as schematically shown in Figure 1. Note that each curvature has a sign: It is positive if the path is convex from one side, negative otherwise, and zero if the path is straight. The mean curvature, H , and the Gaussian curvature, K , are defined as,

$$H = \frac{\kappa_1 + \kappa_2}{2}, \quad K = \kappa_1 \kappa_2 \quad (1)$$

They are uniquely determined at the point \mathbf{p} and characterize the local shape of the surface. The sign of K classifies the shape of the surface: it is elliptic, if $K > 0$, parabolic if $K = 0$, and hyperbolic if $K < 0$. Among hyperbolic surfaces, if $H = 0$ everywhere on the surface, it is a “minimal surface”. We will first describe the principle of the curvature measurements in the following section and later discuss in detail the image processing.

A parallel surface to the interface is formed by translating the original interface along its normal by an equal

- (21) Kawakatsu, T.; Kawasaki, K.; Furusaka, M.; Okabayashi, H.; Kanaya, T. *J. Chem. Phys.* **1993**, *99*, 8200.
- (22) Besl, P. J.; Jain, R. C. *Comput. Vision Graph. Image Process.* **1986**, *33*, 33.
- (23) Bullard, J. W.; Garboczi, E. J.; Carter, W. C.; Fuller Jr., E. R. *Comput. Mater. Sci.* **1995**, *4*, 103.
- (24) Jinnai, H.; Nishikawa, Y.; Koga, T.; Hashimoto, T. *Macromolecules* **1995**, *28*, 4782.
- (25) Jinnai, H.; Koga, T.; Nishikawa, Y.; Hashimoto, T. *Phys. Rev. Lett.* **1997**, *78*, 2248.
- (26) Wilson, T. *Confocal Microscopy*; Academic Press: London, 1990.
- (27) Hilbert, D.; Cohn-Vossen, S. *Geometry and the Imagination*; Chelsea Publishers: New York, 1952.

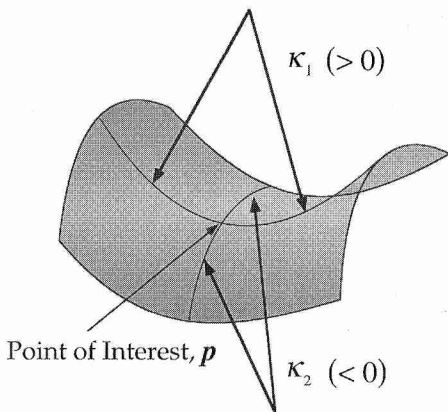


Figure 1. Definition of the surface curvatures. The principal curvatures at a point on the surface are defined as the maximum and minimum curvatures. Note that the curvature is signed: the curvature is positive for the case where the center of the radius of the curvature is placed in one side and negative for the other side.

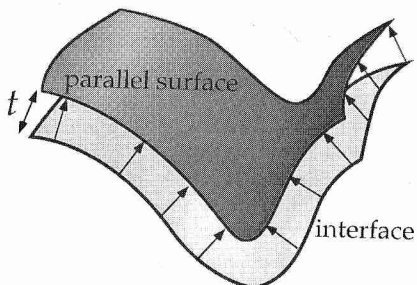


Figure 2. Parallel surface with the displacement t from the interface.

distance everywhere on the surface, as schematically depicted in Figure 2. The relation between the area of the infinitesimal patch at a point \mathbf{p} , $da(0, \mathbf{p})$, and that of the parallel patch, $da(t, \mathbf{p})$, is²⁸

$$da(t, \mathbf{p}) = da(0, \mathbf{p})(1 + 2H(\mathbf{p})t + K(\mathbf{p})t^2) \quad (2)$$

where $H(\mathbf{p})$ and $K(\mathbf{p})$ are, respectively, the mean and Gaussian curvatures at the point \mathbf{p} and t is a signed displacement of the parallel surface from the interface: it is positive if the direction of the displacement points to one side of the surface, and negative otherwise. Summing eq 2 over the whole area of the interface by changing the position of the point of interest, \mathbf{p} , gives

$$A(t) = A(0)(1 + 2\langle H \rangle t + \langle K \rangle t^2) \quad (3)$$

where $A(t) \equiv \int_p da(t, \mathbf{p})$, $A(0)$ is the total area of the original interface, and $A(t)$ is that of the parallel surface at the displacement t . The curvatures, $\langle H \rangle$ and $\langle K \rangle$, are expressed as

$$\langle H \rangle = \frac{\int_p H(\mathbf{p}) da(0, \mathbf{p})}{\int_p da(0, \mathbf{p})}, \quad \langle K \rangle = \frac{\int_p K(\mathbf{p}) da(0, \mathbf{p})}{\int_p da(0, \mathbf{p})} \quad (4)$$

Thus, the $\langle H \rangle$ and $\langle K \rangle$ are the *area-averaged* quantities. According to eq 3, $\langle H \rangle$ and $\langle K \rangle$ can be deduced from the area variation of parallel surface with the parallel displacement t as a variant.

(28) Hyde, S. T. *J. Phys. Chem.* **1989**, *93*, 1458.

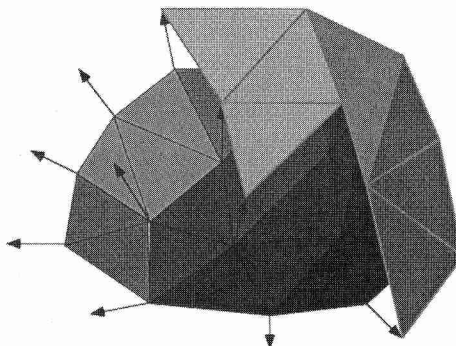


Figure 3. Construction of the parallel surface. The parallel surface is the assembly of the polygons connected to the head of each of the displacement vectors (parallel to normals, and everywhere of equal length) while the origins of the displacement vectors are located at the corresponding vertices of the interface.

3. Scheme of Measurement

3.1. Construction of the Parallel Surface. In general, a 3D image is constructed from a data set of a series of 2D slices with a certain separation distance, i.e., a 3D array of data, which is commonly used not only for LSCM but also for the computer tomography, magnetic resonance imaging, and so on. In the case of LSCM,²⁵ for example, the image contrast corresponds to the concentration of fluorescent molecules that are chemically attached to one of the constituents. One can assign an interface between the regions that are rich in the labeled molecules and the depleted regions by defining an appropriate threshold value. That is to say, one assigns unity if the data value is greater than the threshold, while zero otherwise.

The *marching cubes algorithm* (MCA)²⁹ was used to find the interface. In this algorithm, a cube was created from eight pixels; four each from two adjacent slices. The interface intersects those cube edges where intensity of one vertex is larger than the threshold, e.g., outside the interface, and the other is below, e.g., inside the interface. Depending on the combination of such inside and outside vertices among the eight, the location of the interface in the cube can be determined. Note that MCA defines 14 different surface-edge intersections if one takes rotation and mirror symmetries into consideration (see Figure 3 of ref 29). This gives a polygonal representation of the interface, which eventually reduces to triangles, from the 3D array of data by the MCA, the normal vector of each triangle, \mathbf{n}_{tri} , can be estimated by

$$\mathbf{n}_{tri} = \frac{(\mathbf{p}_2 - \mathbf{p}_1) \times (\mathbf{p}_3 - \mathbf{p}_2)}{|(\mathbf{p}_2 - \mathbf{p}_1) \times (\mathbf{p}_3 - \mathbf{p}_2)|} \quad (5)$$

where \mathbf{p}_1 , \mathbf{p}_2 , and \mathbf{p}_3 are the coordinates of the vertices of the triangle.

The normal vectors thus obtained from the MCA were used to evaluate normal vectors at vertices of the polygon, \mathbf{n} . We note that the normal vectors obtained by the MCA, i.e., \mathbf{n}_{tri} , were those for the triangles comprising the polygon, not for the vertices. \mathbf{n} was estimated by averaging the normal vectors of the neighboring triangles that shared the vertex of interest with those areas as a weighting

(29) Lorensen, W. E.; Cline, H. E. *Computer Graphics, SIGGRAPH '87* **1987**, *21*, 163.

$$\mathbf{n} = \frac{\sum_i S_i \mathbf{n}_{\text{tri}}^i}{\left| \sum_i S_i \mathbf{n}_{\text{tri}}^i \right|} \quad (6)$$

Here $\mathbf{n}_{\text{tri}}^i$ and S_i denote, respectively, the normal vector and the area of i th neighboring triangle.

Following eq 3, the parallel surface which will be used for the curvature measurements was computationally created as schematically shown in Figure 3. Displacement vectors with length t , \mathbf{t} , at the each vertex are defined by $\mathbf{t} = t\mathbf{n}$ by using the normal vectors estimated by the above scheme at each vertex of the triangles. Connecting the top of the displacement vectors makes a imaginary surface parallel to the interface ("parallel surface"). The area of the parallel surface at t , $A(t)$, was obtained by summing up areas of all the triangles that consist of the parallel surface.

3.2. Introduction of Negative Surface Area. In some cases, the area of the parallel surface has to be assigned a "negative" value. Suppose the interface is characterized by principal curvatures $1/r_1 (= \kappa_1)$ and $1/r_2 (= \kappa_2)$. Thus, $H = (1/r_1 + 1/r_2)/2$ and $K = 1/(r_1 r_2)$. Substituting these curvatures into eq 3 gives

$$A(t) = \frac{A(0)}{r_1 r_2} (t + r_1)(t + r_2) \quad (7)$$

For example, let us consider the case of $0 < r_1 < r_2$. If $t < -r_1$, the sign of $(t + r_1)$ becomes negative, so that the area of the parallel surface, $A(t)$, also becomes negative. Such an example is schematically shown in Figure 4, in which the parallel surface has a "cusp" and turns "inside-out". Such regions of negative area were accounted for as follows.

Because the interface is eventually expressed as an assembly of triangles, we consider for convenience one such triangles. Let the position vector of the vertices of the triangle be $\mathbf{p}_1(t)$, $\mathbf{p}_2(t)$, and $\mathbf{p}_3(t)$. Using the area vector of the triangle, $\mathbf{A}_{\text{tri}}(t)$, given by

$$\mathbf{A}_{\text{tri}}(t) = \frac{1}{2}[(\mathbf{p}_2(t) - \mathbf{p}_1(t)) \times (\mathbf{p}_3(t) - \mathbf{p}_2(t))] \quad (8)$$

the signed area of the triangle, $A_{\text{tri}}(t)$, is defined by

$$A_{\text{tri}}(t) \equiv \text{sgn}[\mathbf{A}_{\text{tri}}(t) \cdot \mathbf{A}_{\text{tri}}(0)] |\mathbf{A}_{\text{tri}}(t)| \quad (9)$$

where the first part of eq 9 represents the sign of the area, which is positive if the direction of $\mathbf{A}_{\text{tri}}(t)$ is same as that of $\mathbf{A}_{\text{tri}}(0)$, i.e., $\mathbf{A}_{\text{tri}}(t) \cdot \mathbf{A}_{\text{tri}}(0) > 0$, and vice versa.

On the basis of eq 3, $\langle H \rangle$ and $\langle K \rangle$ can be determined by measuring $A(t)$ with various t . We refer to this scheme as the "parallel surface method (PSM)".

4. Application of PSM and Discussion

4.1. Application of PSM to a Model Bicontinuous Structure. The PSM was first applied to simple objects such as spheres and cylinders, which gave good agreement with the analytically calculated curvatures (see Appendix). The precision of the PSM was further checked by measuring curvatures of a bicontinuous interface with known $\langle H \rangle$ and $\langle K \rangle$, the gyroid, which is one of many periodic minimal surface structures known to date. Figure 5a shows an approximation to the gyroid, generated by

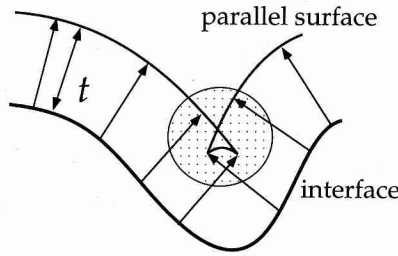


Figure 4. Folding of the parallel surface due to large displacement beyond the radii of the surface curvatures.

using the trigonometric approximation:^{30,31}

$$f(x,y,z) = \sin \frac{2\pi x}{L} \cos \frac{2\pi y}{L} + \sin \frac{2\pi y}{L} \cos \frac{2\pi z}{L} + \sin \frac{2\pi z}{L} \cos \frac{2\pi x}{L} \quad (10)$$

where L is the conventional unit cell edge of the gyroid. The interface of the gyroid is characterized by $f(x,y,z) = 0$. The interface divides whole space into two subparts: shown in Figure 5a, one side of the interface colored by dark gray faces pointing into the subphase containing one constituent (say, A) and the other side colored by the light gray, pointing to the other component (say, B). The arguments of eq 10 are integers, $x,y,z = 0, 1, 2, \dots, D$. The length of the edge of the 3D image corresponds to D . For the measurements in the present section, D was set to be equal to L , i.e., $D = L$. So we obtained the 3D images of D^3 pixel³ including one crystallographic unit cell. As described later, accuracy of the measurements depends on the quality of the 3D image, i.e., roughness of the interface.

Figure 5b shows an example of the PSM measurement for the gyroid ($D = L = 32$ pixels). $A(t)$ was plotted as a function of t . As predicted by eq 3, $A(t)$ was a parabola. The best-fit of eq 3 gave $\langle K \rangle \approx -0.0154 \text{ pixel}^{-2} = -15.8L^{-2}$ and $\langle H \rangle \approx 0L^{-1}$, which reasonably agrees with the analytical value of $\langle K \rangle \approx -16.2L^{-2}$ and $\langle H \rangle = 0L^{-1}$.^{32,33}

Figure 6 demonstrates how the roughness of the interface affects the accuracy of the measurements. The PSM has been applied to various sizes, that is various D , of the 3D image of the gyroid. Each 3D image contains one crystallographic unit cell. The area-averaged principal curvatures are calculated from

$$\langle \kappa_1 \rangle \equiv \langle H \rangle + \sqrt{\langle H \rangle^2 - \langle K \rangle}$$

and

$$\langle \kappa_2 \rangle \equiv \langle H \rangle - \sqrt{\langle H \rangle^2 - \langle K \rangle}$$

which are plotted against D in Figure 6. The ideal values for the gyroid are³⁴

$$\langle \kappa_1 \rangle = -\langle \kappa_2 \rangle = \sqrt{16.2/L} (= \sqrt{16.2/D})$$

(30) Nishikawa, Y.; Hasegawa, H.; Hashimoto, T.; Hyde, S. T. In preparation.

(31) Barnes, I. S.; Hyde, S. T.; Ninham, B. W. *J. Phys. (France) Colloq.* 1990, supplement to 51, C7–19.

(32) Hyde, S. T. *Langmuir* 1997, 13, 842.

(33) In ref 32, after a certain transformation,

$$\langle K \rangle = -\left(\frac{1}{H} \frac{\chi}{V}\right)^{2/3}$$

is obtained. For gyroid, $H \approx 0.7665$ and $\chi = -8$ in a crystallographic unit cell. Thus $\langle K \rangle \approx -16.2L^{-2}$ per unit cell.

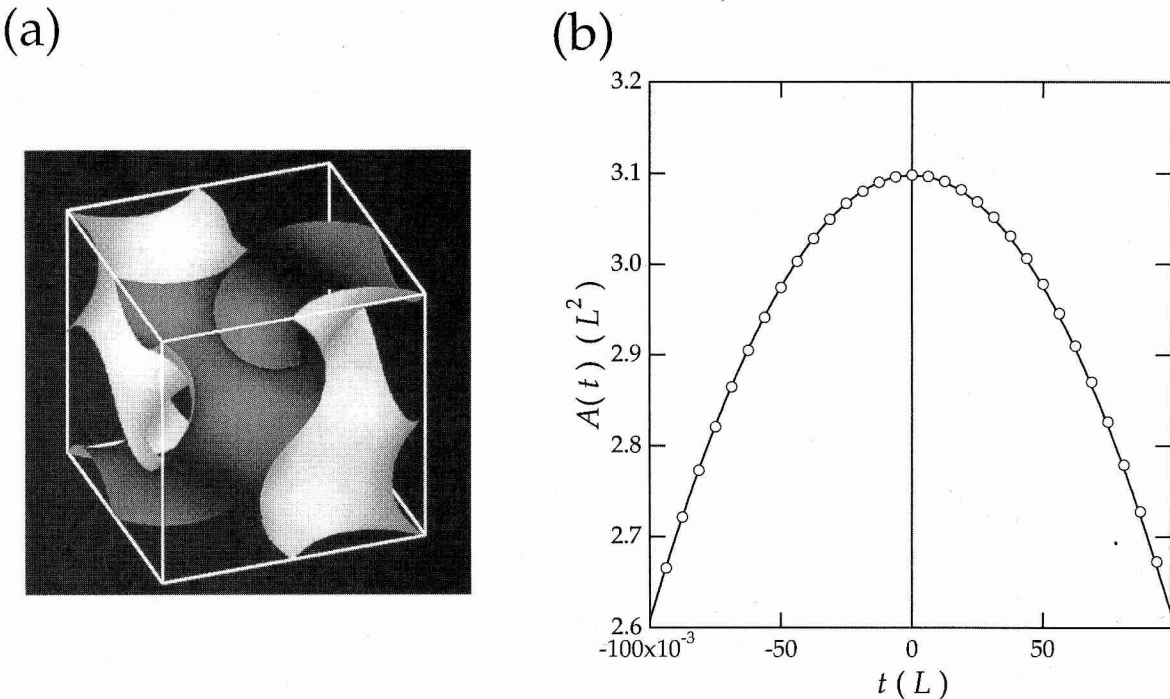


Figure 5. (a) 3D view of gyroid, containing a single conventional crystallographic unit cell. (b) Plot of the area of the parallel surfaces against the displacements. The image of gyroid with the periodic length $L = 32$ pixels was subjected to the measurement. The solid line represents the best-fit of eq 3 and the fitting gave $\langle H \rangle \cong 0L^{-1}$ and $\langle K \rangle \cong -15.8L^{-2}$.

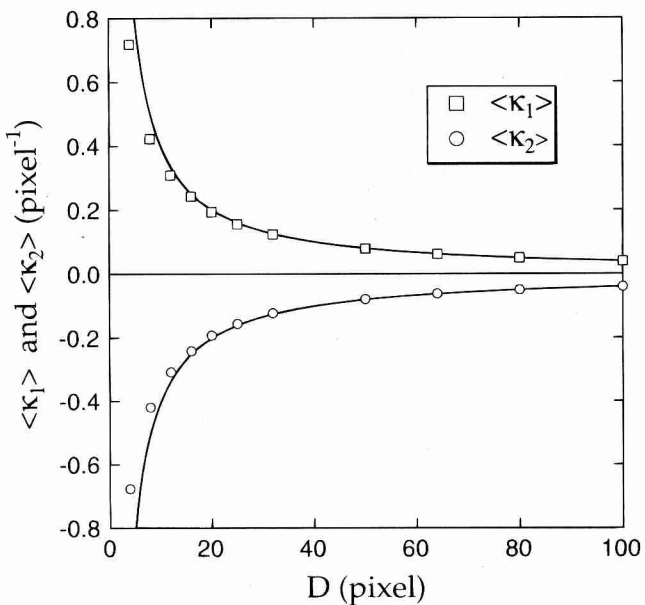


Figure 6. Plot of the area-averaged principal curvatures, κ_1 and κ_2 , obtained from PSM versus the length of the edge of the 3D image of gyroid, D . The solid lines are the analytically calculated principal curvatures.

which are shown by solid lines in the figure. The measured principle curvatures agreed well with the predicted value; the maximum error observed was ± 0.3 pixel\$^{-1}\$ in the case of $D = 4$. As D becomes larger, the accuracy improves. This is because the interface of the gyroid consisted of a larger number of triangles as D increased.

In order to measure the roughness of the interface, we introduce an index, RI defined by

$$RI = \sqrt{\langle A_{\text{tri}} \rangle^{-1} (\langle \kappa_1 \rangle + |\langle \kappa_2 \rangle|)} \quad (11)$$

where $\langle A_{\text{tri}} \rangle$ denotes the average area of each triangle

$$\langle A_{\text{tri}} \rangle \equiv \sum_i |A_{\text{tri}}^i| / N$$

and A_{tri}^i is the area of the i th triangle and N is total number of triangles. RI gives a measure of relative roughness of the interface constructed by triangles relative to the averaged curvature. The smaller the RI value, the smoother the constructed interface becomes. Note that square root of the area of a triangle and the average curvature have, respectively, dimensions of length and reciprocal length, and hence the index is a dimensionless quantity. In the case of the gyroid, for example, RI was 0.10 for $D = 32$ pixels. The range of RI of the data plotted in Figure 6 was from 0.03 ($D = 100$) to 0.82 ($D = 4$). Hence, we conclude that the PSM technique allows estimation of the interfacial curvatures of the hyperbolic surface within the uncertainty of 5% up to RI = 0.27 ($D = 12$). Similar precision checks have been done for the sphere and the cylinder, described in the Appendix. The sphere and the cylinder gave $\pm 5\%$ error up to RI = 0.27 and 0.20, respectively. Therefore, we conclude that the PSM is capable of measuring the interfacial curvatures within 5% error up to RI = 0.20 for any surface.

4.2. Application of PSM to the Bicontinuous Phase-Separated Structure of a Polymer Blend. A 3D image of the bicontinuous phase-separated structure of a mixture of poly(styrene-*ran*-butadiene) (SBR) and polybutadiene (PB) in the late stage of SD was experimentally observed by LSCM.²⁵ The image was constructed by 60 slices of 100 pixel \times 100 pixel 2D images (0.625 $\mu\text{m}/\text{pixel}$). The resulting interface between the SBR-rich and PB-rich subphases are displayed in Figure 7. PSM was applied to the interface, which yielded $\langle K \rangle = -0.024$ pixel\$^{-2} = -9.08L^{-2}\$ and $\langle H \rangle = 0.0044$ pixel\$^{-1} = 0.05L^{-1} (see Figure 3 of ref 25). Note that the wavelength of the

(34) $\langle K \rangle = -16.2L^{-2}$ and $H = 0$ give $\langle \kappa_1 \rangle = -\langle \kappa_2 \rangle = -\langle K \rangle^{1/2} = 16.2^{1/2}/L$.

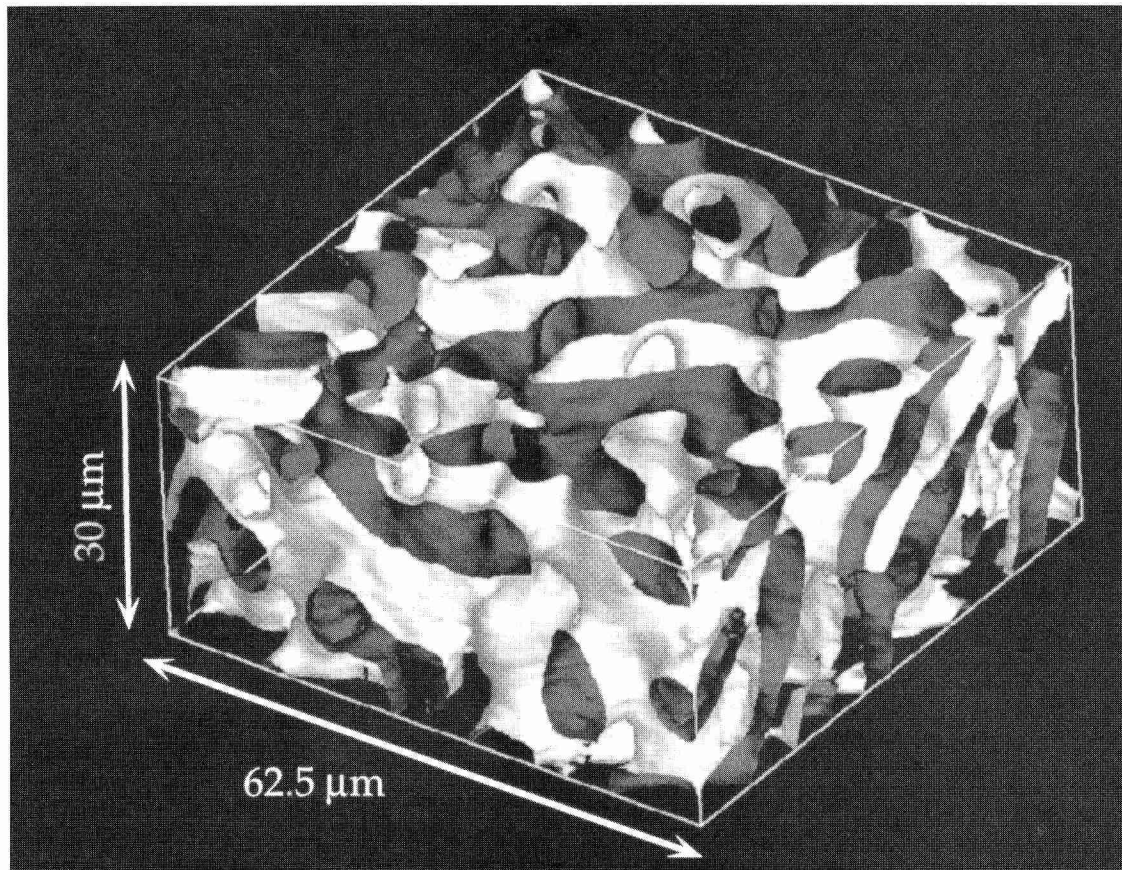


Figure 7. 3D reconstruction of the bicontinuous phase-separated structure of the SBR/PB blends observed by LSCM. The volume is $62.5 \times 62.5 \times 30 \mu\text{m}^3$. The PB-rich phase and the SBR-rich phase are filled up to the lighter and darker sides, respectively.

dominant mode of concentration fluctuations, which is defined by $2\pi/q_m$ (q_m is the wavenumber at the maximum intensity of the 3D Fourier transform of density-density correlation function of the 3D image shown in Figure 7), is taken as the unit length, viz. $L = 2\pi q_m$. $\langle k_1 \rangle$ and $\langle k_2 \rangle$ calculated from the curvatures were, respectively, 3.06 and $-2.96L^{-1}$. The roughness index, RI, was 0.12, which is well within the measurable range of the PSM. The obtained negative $\langle K \rangle$ clearly demonstrates that the interface of the bicontinuous structure, on average, consists of a hyperbolic surface. In other words, the principal curvatures at a point of interest have opposite signs, i.e., anticlastic. The small positive value of the mean curvature may not be significant, as the absolute value of the area-averaged radii of the principal curvatures, $1/|\langle k_1 \rangle|$ and $1/|\langle k_2 \rangle|$, are 6.3 and 6.5 pixels, respectively, and their difference is less than the resolution of the image, i.e., 1 pixel. Therefore, we assume that $\langle H \rangle \approx 0L^{-1}$.

It is important to note here that the two bicontinuous structures subjected to the PSM measurements may be the consequence of completely different physics: the gyroid is often used to model the interface of the microphase-separated block copolymers, i.e., an equilibrium structure, while the SD is a typical nonequilibrium process, and hence the bicontinuous structure realized in this process is a nonequilibrium structure. Yet, both interfaces, polymer

(35) The typical composition of the block copolymer exhibiting the gyroid morphology lies in the range 0.6–0.65, while the volume fraction of the gyroid generated by eq 10 and listed in Table 1 is 0.5. In order for the direct comparison between the gyroid in Table 1 and that observed in block copolymer systems, it is necessary to introduce a “lamination” concept, in which the microdomain interface does not correspond to the minimal surface itself but to the parallel surface. See ref 7 for detail.

Table 1

	polymer blend	gyroid ^a
volume fraction	0.5	0.5
RI	0.12	(0.14)
$\langle K \rangle (L^{-2})$	-9.08	-16.2
A/V (L^{-1})	3.15	3.09
χ	-4.55	-8
HI	1.04	0.7665 ^b
		(0.78)

^a The values in the parentheses are measured by PSM form the 3D image of gyroid shown in Figure 5a. ^b Reference 32.

blends and the minimal surface, have common surface geometry: $\langle K \rangle < 0$ and $\langle H \rangle \approx 0$. An interesting question is whether the bicontinuous interface developed in the SD process—which is close to a minimal surface, since $\langle H \rangle \approx 0$ —resembles triply periodic minimal surfaces formed in equilibrium processes.

Table 1 summarizes quantities obtained as a result of the PSM for the two bicontinuous interfaces.³⁵ The surface-to-volume ratios, A/V, were similar between the bicontinuous phase-separated structure of the polymer blend and the gyroid. However, in order to compare different hyperbolic surfaces, one should take the topology of the interface into account, which is conventionally described by its Euler-Poincaré characteristic, χ , provided the surface is closed. According to the Gauss-Bonnet theorem of differential geometry, χ is related to the Gaussian curvature by²⁷

$$2\pi\chi = \int K da = \langle K \rangle A \quad (12)$$

χ characterizes the complexity in the connectivity of the

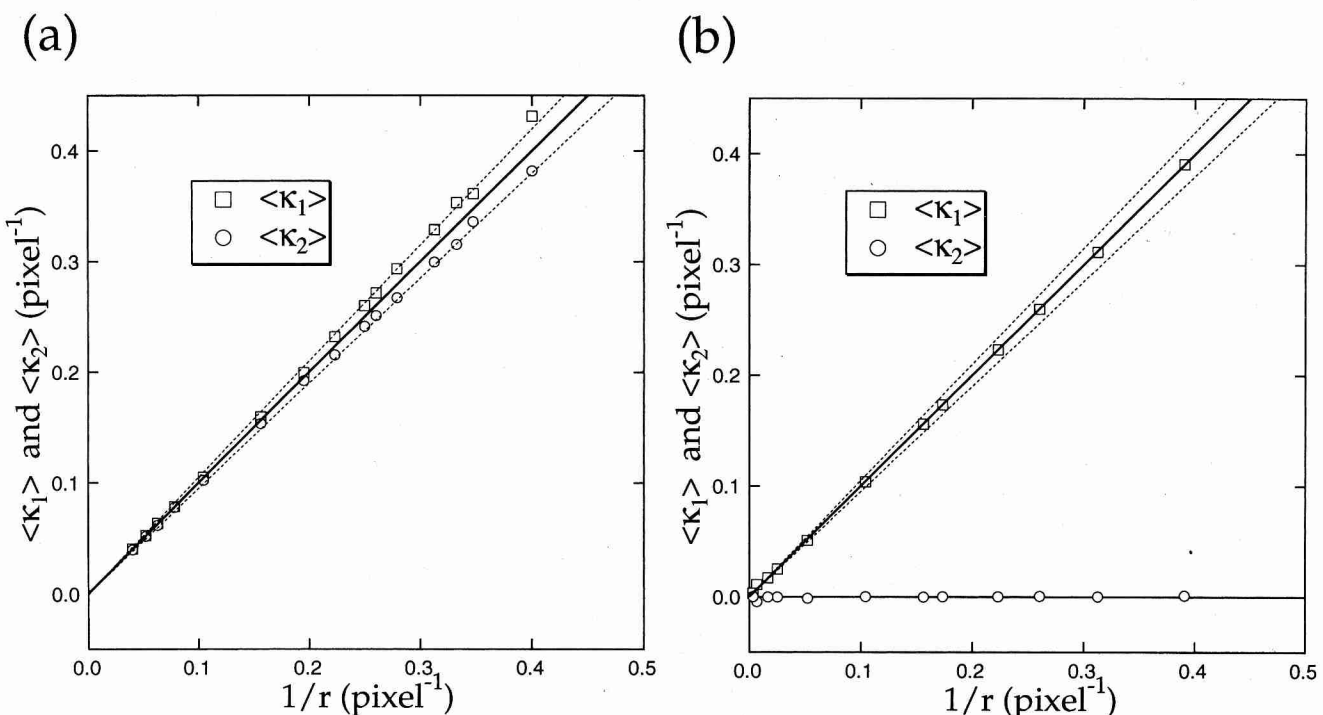


Figure 8. Results of the PSM for (a) spheres and (b) cylinders with various radii. The principal curvatures, κ_1 and κ_2 , calculated from the measured H and K are plotted against the reciprocal number of the radii of the model shapes. The dotted lines represent the curvatures with $\pm 5\%$ error in the radius of the curvature. The solid lines are the analytically calculated principal curvatures.

network: the more negative χ becomes, the more complex the structure is.³⁶ χ of the polymer blend was -4.55 , as listed in Table 1. This means that the topological complexity of the bicontinuous interface of the polymer blend was close to that of a sphere with three handles ($\chi = -4$) in L^3 .

A useful dimensionless measure of the surface form of bicontinuous shapes is the homogeneity index, HI, which combines the surface-to-volume ratio of a hyperbolic surface with its topology:³²

$$\text{HI} \equiv \left\{ -\frac{A^3}{2\pi\chi V^2} \right\}^{1/2} \quad (13)$$

For the “homogeneous” minimal surfaces where K is constant everywhere on the surface, $\text{HI} = 0.75$. In practice, the actual HI for minimal surfaces may scatter around 0.75, e.g., $\text{HI} = 0.7665$ for the gyroid, $\text{HI} = 0.7498$ for the Schwarz D-surface, and $\text{HI} = 0.7163$ for the P-surface.³² The bicontinuous interface of the phase-separated polymer blend gives $\text{HI} = 1.04$ as listed in Table 1, which is 40% larger than 0.75. This means that the bicontinuous interface of the polymer blends differs somewhat from the simple periodic minimal surfaces. In order to be more

(36) The Euler-Poincaré characteristic, χ , is simply related to another topological measure, called “genus”, g , of the surface through the equation $\chi = 2 - 2g$. Note that the relation is valid only for “two-sided” (or “orientable” surfaces) and not for the “one-sided” surfaces such as the Möbius strip. Since, no matter how a surface is stretched or squashed, the χ is not affected by these distortions, any orientable surface is always (topologically) the same as a single sphere that is decorated with some number of handles. A surface with genus g is topologically equivalent to a sphere with g handles: The genus corresponds to the number of handles. The most simple example is that of the convex polyhedra, all of which are equivalent to a sphere, and all having a genus of zero; hence $\chi = 2$. As one adds a handle to a polyhedra and distorts the shape, one gets a doughnut-shape surface (which even includes mugs!). In such a case, $g = 1$, so that $\chi = 0$. Similarly, a pretzel corresponds to a sphere with two handles ($g = 2$); hence, $\chi = -2$. Therefore, as more handles are added to structure and thus the structure gets more complicated, χ gets smaller.

specific, it is necessary to measure the local surface curvatures and the curvature distributions over the surface, rather than the area-averaged curvatures. We will discuss a method to measure the distribution of the curvatures in a subsequent paper of this series in the future.³⁷

5. Conclusion

A method to measure interfacial curvatures from three-dimensional (3D) digital images was developed on the basis of the differential geometry. The method is applicable to a stack of two-dimensional images obtained from laser scanning confocal microscopy (LSCM). The format used for imaging is common to that used for the computer tomography, magnetic resonance imaging, and so on. In the present paper, we focus on the bicontinuous interface between immiscible components in a two-phase composite material. The interface was determined by binarizing images with an appropriate threshold. The method involves generation of imaginary parallel surfaces from the interface as a function of displacement, which was then used with a fundamental equation of differential geometry, i.e., eq 3 (parallel surface method, PSM).

The PSM was applied to a bicontinuous interface which is a minimal surface predicted in differential geometry. The precision of the curvature measurement of the PSM was critically tested by comparing the obtained result with the analytically predicted value. The PSM measured interfacial curvatures within 5% error if an index characterizing interface roughness was less than 0.20 (see eq 11). In addition, the PSM was then applied to an experimentally obtained 3D bicontinuous interface developed during the spinodal decomposition, which clearly showed that the spinodal interface is, on average, anti-elastic.

(37) Nishikawa, Y.; Koga, T.; Jinnai, H.; Hashimoto, T. In preparation.

6. Appendix

The precision of the PSM was extensively tested for spheres and cylinders. The 3D images of the spheres are generated from

$$f(x,y,z) = \sqrt{(x - x_0)^2 + (y - y_0)^2 + (z - z_0)^2} - r \quad (\text{A1})$$

and for cylinders

$$f(x,y,z) = \sqrt{(x - x_0)^2 + (y - y_0)^2} - r \quad (\text{A2})$$

by setting $f(x,y,z) = 0$, where (x_0, y_0, z_0) is the coordinate of

the center of sphere or cylinder and r is the radius. The principal curvatures for a sphere are analytically calculated as $\kappa_1 = \kappa_2 = 1/r$, and for cylinder $\kappa_1 = 1/r$ and $\kappa_2 = 0$. The results of the PSM for the spheres and cylinders with various radii are plotted in Figure 8.

The errors in the measurements increase as the reciprocal of the radius increases. As shown in Figure 8, the PSM can measure the principal curvatures within 5% error for spheres with $r > 3.0$ pixels and for cylinders with $r > 2.0$ pixels. The corresponding RI values of eq 11 for the sphere and the cylinder were 0.27 and 0.20, respectively.

LA970868B